Active gels: dynamics of patterning and self-organization

2006 Phys. Biol. 3 264

(http://iopscience.iop.org/1478-3975/3/4/004)

INSTITUTE OF PHYSICS PUBLISHING PHYSICAL BIOLOGY

Phys. Biol. **3** (2006) 264–273 doi:10.1088/1478-3975/3/4/004

Active gels: dynamics of patterning and self-organization

F Backouche[1], L Haviv[1], D Groswasser[2] and A Bernheim-Groswasser[1]

[1] Department of Chemical Engineering, Ben-Gurion University of the Negev, PO Box 653, Beer-Sheva 84105, Israel
[2] Department of Physics, Ben-Gurion University of the Negev, PO Box 653, Beer-Sheva 84105, Israel

E-mail: bernheim@bgu.ac.il.

Received 9 August 2006
Accepted for publication 14 November 2006
Published 4 December 2006
Online at stacks.iop.org/PhysBio/3/264

Abstract

The actin cytoskeleton is an active gel which constantly remodels during cellular processes such as motility and division. Myosin II molecular motors are involved in this active remodeling process and therefore control the dynamic self-organization of cytoskeletal structures. Due to the complexity of *in vivo* systems, it is hard to investigate the role of myosin II in the reorganization process which determines the resulting cytoskeletal structures. Here we use an *in vitro* model system to show that myosin II actively reorganizes actin into a variety of mesoscopic patterns, but only in the presence of bundling proteins. We find that the nature of the reorganization process is complex, exhibiting patterns and dynamical phenomena not predicted by current theoretical models and not observed in corresponding passive systems (excluding motors). This system generates active networks, asters and even rings depending on motor and bundling protein concentrations. Furthermore, the motors generate the formation of the patterns, but above a critical concentration they can also disassemble them and even totally prevent the polymerization and bundling of actin filaments. These results may suggest that tuning the assembly and disassembly of cytoskeletal structures can be obtained by tuning the local myosin II concentration/activity.

M This article features online multimedia enhancements

1. Introduction

Living cells have remarkable mechanical properties. In addition to passive response to mechanical stresses, eukaryotic cells are also able to actively change their shapes and to generate forces and movement in response to external signals [1, 2]. These properties are mainly attributed to the mechanical and dynamical properties of the cell cytoskeleton. The cytoskeleton is an out-of-equilibrium 3D protein network of polar elastic filaments constantly remodeling via a large number of associate proteins interacting with the cytoskeletal filaments. The cells use these associated proteins to control the filaments' length and spatial organization for regulating active cellular processes such as cell movement and division. Some cellular processes [3] are driven solely by filament polymerization and depolymerization [4]. Other reorganization processes of the cytoskeleton architecture also involve molecular motor proteins [5] interacting with the cytoskeletal filaments, which can polymerize and depolymerize. Molecular motor proteins hydrolyze ATP to generate a driving force and movement along filaments in a direction determined by the filaments' polarity. In the cell, some motors transport cargos along F-actin and microtubules, while others are able to generate relative movement between filaments; this can give rise to complex structural and dynamical self-organization phenomena [6–12].

Myosin II motors play a central role in active remodeling of the actin cytoskeleton and in the self-organization of cytoskeletal structures [6–10, 12]. These motors have a unique property to spontaneously self-assemble into small motor aggregates commonly named 'minifilaments' [13]. These active crosslinkers can simultaneously interact with a number

of actin filaments and move toward their 'plus' end in the presence of ATP. Myosin II motors are present in many cellular processes that require substantial structural rearrangements of the actin cytoskeleton architecture. One of these processes is cellular division, in which myosin II motors participate in the assembly of a contractile ring [14]. Myosin II motors are also required for the assembly of stress fibers [6] and dense active networks [9].

These cytoskeletal networks are viscoelastic materials driven away from equilibrium by ATP hydrolysis. These networks resemble in many aspects polymer solutions or gels. The main difference from usual passive polymer solutions is their intrinsic activity resulting from filament polymerization/depolymerization kinetics or from the action of molecular motors which act as active crosslinkers, constantly breaking and reforming. While the subject of passive, viscoelastic filament solutions has been extensively studied [15–18], active filament-motor systems started to attract attention only recently. These active gels represent a special class of polymeric systems with unusual transient non-equilibrium and mechanical properties [19–21].

The study of the action of individual components involved in the cytoskeleton active remodeling is too complex to be studied *in vivo*. Simplified *in vitro* systems provide a controlled environment for studying systematically the role of constituent proteins [22–29]. The use of *in vitro* systems [22–25, 28, 29] together with novel general theories that predict the formation of steady-state patterns such as bundles, vortices, asters and rotating spirals [30–34] enables us to better understand the mechanism of the active cytoskeleton reorganization by motor proteins. These theoretical studies demonstrate that steady-state patterns are generic and therefore should be experimentally observable in any motor/filament system.

Despite their overwhelming importance, *in vitro* experiments on the active self-organization of actin by myosin II motors are still lacking [35]. In this work, we used a simplified *in vitro* system for exploring the dynamics of actin patterning and self-organization. Here we show that the addition of passive crosslinking proteins is essential for the production of large scale patterns. These results are in accord with other studies demonstrating that actin crosslinking proteins were necessary for actin gel contraction by myosin II motors [36]. We used fascin as the passive crosslinking protein as it has the ability to tightly bundle actin filaments with the same polarity [37, 38], and the reorganization of such bundles by myosin II can be resolved optically.

2. Materials and methods

2.1. Protein purification

Actin was purified from rabbit skeletal muscle acetone powder [39]. Purification of myosin II skeletal muscle was done according to standard protocols [40]. Recombinant fascin [41] was expressed in *E. coli* as a GST fusion proteins. Actin labeled on Cys374 with Alexa 568, or Rhodamin-actin purchased from Cytoskeleton Co. NEM *N*-ethylmaleimide (Sigma Co.) inactivated myosin was prepared according to standard protocols kindly given by T D Pollard (Yale University).

2.2. Motility medium

The motility medium contained 10 mM HEPES, pH = 7.67, 1.7 mM Mg-ATP, 5.5 mM DTT, 0.12 mM Dabco (1,4-diazabicyclo[2,2,2]octane), 0.13 M KCl, 1.6 mM $MgCl_2$, 1% BSA, an ATP regenerating system 0.1 mg ml^{-1} creatine kinase and 1 mM creatine phosphate and various concentrations of G-actin, myosin II and fascin.

2.3. Optical microscopy and experimental procedure

Actin assembly was monitored by fluorescence using an Olympus 71× microscope (Olympus Co., Japan). Time-lapse images were acquired using a Coolsnap HQ camera (Photometrics Co.) or an Andor DV887 EMCCD camera (Andor Co., UK). Data acquisition and analysis was performed using METAMORPH (Universal Imaging Co.). To prevent protein adsorption, the glass coverslips were coated with an inert polymer (PEG-mal, Nectar Co.) according to a standard protocol [42].

3. Results

3.1. Dynamics of local features inherent to myosin II activity

In figure 1, we focus on the formation dynamics of local features inherent to myosin II activity in order to understand the formation dynamics of the global pattern/active gel. In figure 1(*a*), we follow the formation of a single junction (defined as an 'aster junction' (AJ)). This AJ is formed by the transportation of actin–fascin/bundles, AFBs (marked by a white arrow-head), along other 'track' AFBs (marked by a gray arrow-head) toward a junction point (marked by a white arrow). The last snapshot shows that the junction comprised of eight AFBs transported to the junction point along 'track' AFBs from the network residing below (see also movie 1 available at stacks.iop.org/PhysBio/3/264). Myosin II motors are 'plus' end motors; according to this, the 'plus' ends of the transported AFBs are pointing toward the junction center. Figure 1(*b*) shows bundling of AFBs by myosin II; the upper AFB (marked by a white arrow) slides toward the fixed AFB (gray arrow), resulting in a thicker bundle. The forces exerted by myosin II heads are sufficient not only to transport bundles but also to bend them (figure 1(*c*)). Here, the arrows mark the connection point between the two AFBs. The transported bundle, marked by dashed gray lines, is anchored at its two ends (arrowheads) to the surrounding network and, as a result, the bundle bends.

3.2. Phase diagram of large scale patterns generated by myosin II motors in the presence of fascin on short time scales

The molecular forces and movements generated at the local scale by myosin II motors determine the dynamics of patterning and self-organization of the global system (or

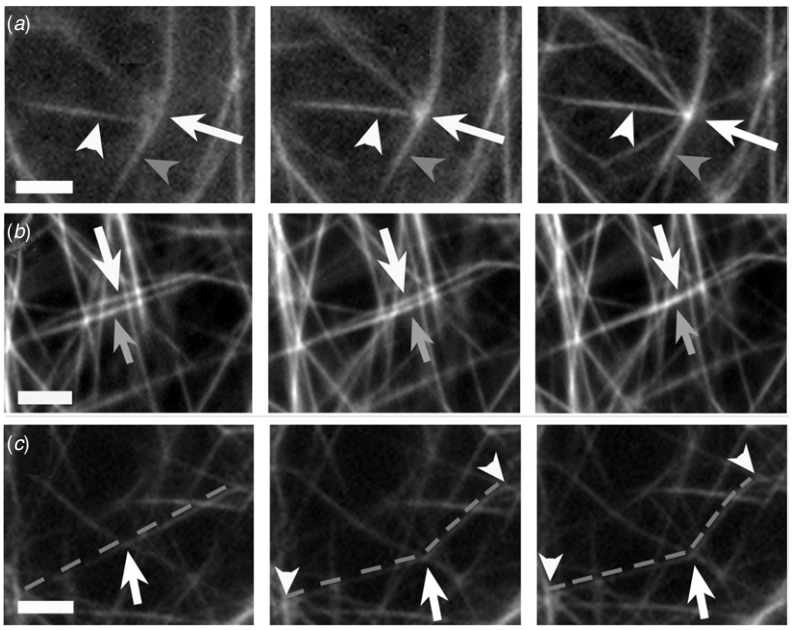

Figure 1. Active network self-organization: small scale dynamics inherent to myosin II activity. (*a*) Formation of a junction by translocation of AFBs to the meeting point. Conditions: 21 μm [A], [F]/[A] = 0.05 and [M]/[A] = 0.05. Δt (left to right): 2.5 min and 6 min. (*b*) AFBs' bundling by myosin II. Conditions as in (*a*). (*c*) AFB deformation during myosin II translocation. Conditions: 15 μM [A], [F]/[A] = 0.14 and [M]/[A] = 0.056. Δt = 45 s. (*a*)–(*c*) Bar = 5 μm.

active gel) at large scales. The self-organization process of these active gels takes place in several steps, each on a typical time scale. The first step of the process is actin filament polymerization/bundling. Bundling and polymerization happen concomitantly. We start observing bundles after only a few minutes (2–5 min). Since only bundles can be optically resolved, we assume that individual actin filaments also polymerize in parallel. The second step starts after the bundles grow long enough to overlap; only then can motor aggregates generate relative motion. Typically, large scale patterns reach a steady state[3] 15–60 min after mixing, depending on the pattern type and the degree of connectivity. In turn, the nature of the patterns depends on the concentrations of fascin and myosin II motors in the motility medium. This stage can take up to 1 h in the case of disconnected asters and less than 15 min in the case of highly connected rigid networks (figure 2 caption). In general, in the case of connected structures the duration of this stage depends on the time it takes for the active gel to reach mechanical equilibrium, whereas in the case of disconnected structures it can be due to the depletion of actin bundles from the bulk. Occasionally, a third step is observed; this occurs after reaching steady state and is characterized by a significant structural change. In structures such as rings and asters this change appears as 'novas' and in structure such as networks, the global network structure deforms.

In figure 2, we present a phase diagram showing different types of patterns at the steady state (up to 1 h). We examined the myosin II/actin system in the absence of fascin ([fascin]/G-actin] = [F]/[A] = 0) by scanning the myosin concentration from 100 nM to 4 μM and observed a 'homogeneous solution' without any mesoscopic patterns (data not shown). After fascin was added, large scale structures appeared. The activity of the motor heads is crucial for the reorganization process; the use of inactivated NEM myosin II motors (see section 1) prohibited any pattern formation, signifying that the ATPase activity of the motors is indispensable for the patterning and the self-organization process.

The resulting patterns depend on the motor and bundling protein concentrations. Without motors ([myosin II]/G-actin] = [M]/[A] = 0), entangled 'passive networks' of AFBs are observed (figures 2(*a*), (*e*) and (*i*)). These are passive networks that are well documented in the literature [43]. At low fascin concentrations, i.e., [F]/[A] = 0.05, the network is generally isotropic (figure 2(*a*)). At [F]/[A] = 0.1, one observes occasional bundle assemblies in the network (arrows, figure 2(*e*)). Further increase in the fascin concentration to [F]/[A] = 0.14 generates regions of condensed actin bundles (arrows, figure 2(*i*)) and voids.

The addition of motor proteins creates an active system, exhibiting a variety of patterns as well as dynamical phenomena not observed in corresponding passive systems. At fascin concentrations of [F]/[A] = 0.05 and variable [M]/[A] ratios, the motors induced the formation of rings and other one-dimensional (1D) curved structures that are self-organized from the surrounding AFBs network (figures 2(*b*)–(*d*)). At low motor concentrations of [M]/[A] = 0.03 we observe rings of diameter $D \sim 10$ μm, although at low abundance

[3] Since the system can further evolve in time ('novas' and networks transformation) the initial state that the system reaches can be considered as a pseudo-steady state, or more appropriate to define as a mechanically stable state and not a real steady state.

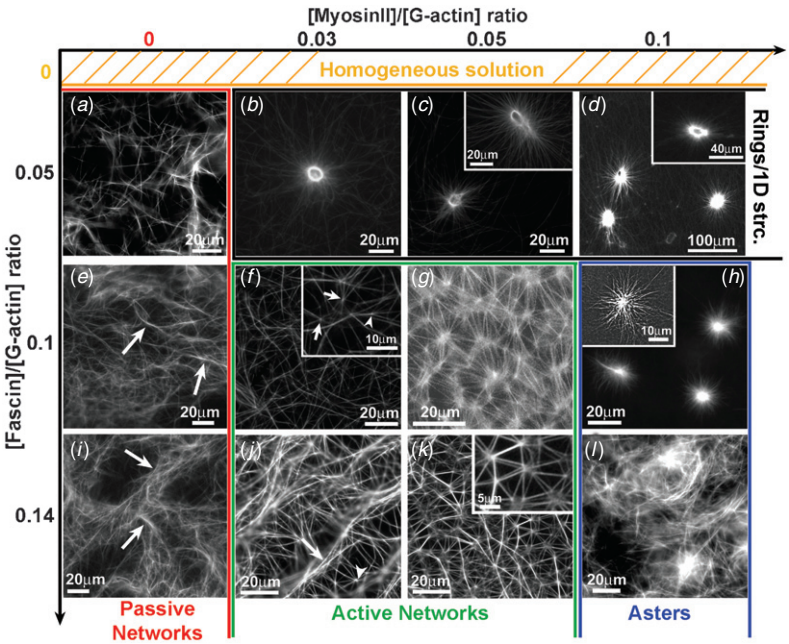

Figure 2. Phase diagram of the patterns generated by myosin II motors in the presence of fascin on short time scales. Actin self-organization was visualized by fluorescence microscopy. Each colored line delimits a region in the phase diagram in which a certain type of pattern or phase exists. Composition: [G-actin] = [A] = 21 μM, and variable ratios of [M]/[A] and [F]/[A]. ((*a*) to (*d*)) [F]/[A] = 0.05 and [M]/[A] ratio is (*a*) 0, (*b*) 0.03, (*c*) 0.05 and (*d*) 0.1. ((*e*) to (*h*)) [F]/[A] = 0.1 and [M]/[A] ratio is (*e*) 0, (*f*) 0.03 (*g*) 0.05 and (*h*) 0.1. ((*i*) to (*l*)) [F]/[A] = 0.14 and [M]/[A] is (*i*) 0, (*j*) 0.03 (*k*) 0.05 and (*l*) 0.1. The reorganization time scale for the formation of passive networks is typically less than 10 min. For active networks the reorganization time ranges from 15 min to 30 min. Under the conditions reported in this phase diagram, the reorganization time for rings/1D structures embedded in a surrounding network is from 20 min to 30 min. For disconnected asters, the typical reorganization time ranges from 40 min to about 1 h.

(figure 2(*b*)). Elevating the [M]/[A] to 0.05 resulted in the formation of a variety of 1D structures including rings (figure 2(*c*)) and ropes (inset, figure 2(*c*)). A further increase in myosin II concentration to [M]/[A] = 0.1 led to the formation of thicker and larger rings of $D \sim 20$–30 μm (figure 2(*d*)). The rings in figure 2(*d*) seem to be full due to a deliberate enhancement of the contrast in order to demonstrate the surrounding network and the AFBs emanating from the ring annulus. The inset in figure 2(*d*) is taken at lower contrast and the ring shape is now clearly observed.

At [F]/[A] = 0.1 and [M]/[A] < 0.1 'active networks' of AFBs are the dominating patterns. Figure 2(*f*) shows a dilute network created at relatively low fascin ([F]/[A] = 0.1) and myosin II ([M]/[A] = 0.03) concentrations. Here we identify some of the actions of myosin II motors on the network. The crosslinking of a few bundles by myosin II produces junctions (arrows, inset); we also detect bundles splitting (arrowhead, inset). Increasing motor concentration to [M]/[A] = 0.05 generates a high-density triangular crosslinked network (figure 2(*g*)). The typical distance between two junctions is 13.0 ± 5.1 μm. Keeping the fascin content constant at [F]/[A] = 0.1 while increasing motor concentration to [M]/[A] = 0.1 resulted in the breakage of the network and in the formation of individual asters (figure 2(*h*)). Myosin II motors move toward the 'plus' end of the AFB, resulting in their accumulation in the aster center; therefore the actin filaments' 'plus' ends are also directed toward the aster core. This is analogous to the polarity of the asters in the MT/kinesin system [23].

The third row in figure 2 is taken at a constant ratio of [F]/[A] = 0.14. 'Active networks' (figures 2(*j*) and (*k*)) are again the dominating structures but are composed of thicker AFBs. Very often the bundles continue to assemble and form regions of condensed AFB assemblies (arrows, figures 2(*i*) and (*j*)), most probably due to the presence of free fascin in the solution. The effect of myosin II on the network structure is revealed when increasing the myosin II concentration to [M]/[A] = 0.05. We see that the regions of condensed bundle assemblies are disentangled and a highly dense triangular crosslinked network is formed (figure 2(*k*)). We noted that increasing [F]/[A] from 0.1 (figure 2(*g*)) to 0.14 (figure 2(*k*)) reduces the inter-junction distance to 9.0 ± 4.1 μm.

Finally, increasing the myosin II concentration to [M]/[A] = 0.1 resulted in the formation of large asters ($D \sim$ 20 μm) embedded in the surrounding network (figure 2(*l*)). This network of asters formed within few minutes, but was unstable and disassembled several minutes later into long (∼20–40 μm) individual AFBs. In the following, these AFBs continue to disassemble, ending up in short (<5 μm) and thin actin filaments/bundles (see the supplementary figure available at stacks.iop.org/PhysBio/3/264). At [M]/[A] > 0.1 we did not even detect actin bundles, meaning that the myosin

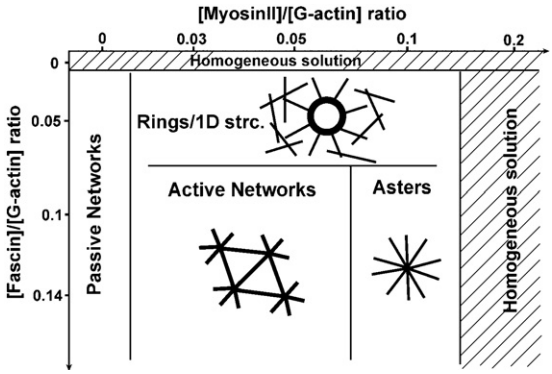

Figure 3. To summarize our findings we present a schematic phase diagram exhibiting the four essential types of patterns (i.e., 'passive networks', 'rings and 1D curve structures' embedded in a surrounding network, 'asters' and 'active networks') formed *in vitro* at short time scales as a function of [F]/[A] and [M]/[A] ratios. Patterns do not form at high concentrations of motors or in the absence of fascin (we called these regions 'homogeneous solutions'). For clarity, schematic drawings of the patterns appear in the appropriate regions of the phase diagram where the lines mark the approximate boundaries between the phases.

II motors inhibit AFBs formation and growth. These findings are summarized in figure 3.

3.3. Patterns' dynamics

The reorganization dynamics characterizing active actin/myosin II solutions are strikingly different from those encountered in passive actin solutions. Passive actin solutions are equilibrium systems; this signifies that the patterns generated do not further evolve in time after being formed. In contrast, active gels are out-of-equilibrium systems driven by motors toward the steady state. The time scale of the dynamic reorganization process depends on the pattern type. For example, structures such as rings and asters as well as dense active networks, which initially reorganize on time scales of 15–60 min (figure 2), undergo further significant global structural transformations at longer time scales.

3.3.1. Evolution dynamics and novas of rings and asters. Whereas asters have a 3D symmetry and look the same regardless of their orientation, rings have a 2D symmetry, and if they are not parallel to the surface, they appear as open structures. Additionally, the rings are not always 'perfect' and their fluorescence distribution is therefore not symmetric. This can possibly be the case of the ring shown in figure 4. Figures 4(*a*)–(*d*) show the ring at consecutive evolution stages (see also movie 3 available at stacks.iop.org/PhysBio/3/264). In figure 4(*e*) we follow the temporal evolution of the ring by measuring the fluorescence intensity of the labeled actin. The process starts with polymerization and bundling of actin filaments and early reorganization processes in segment 1–2. The next step, in segment 2–3, is characterized by a jump in the fluorescence intensity (rate of intensity increase of 280 au min^{-1}) which is a signature of fast local accumulation of AFBs. The accumulation of actin progresses in segment 3–4 (figure 4(*b*)) until it halts ∼15 min later. At segment 4–5 we detect constant fluorescence intensity; here the ring which is connected to the surrounding network by a large number

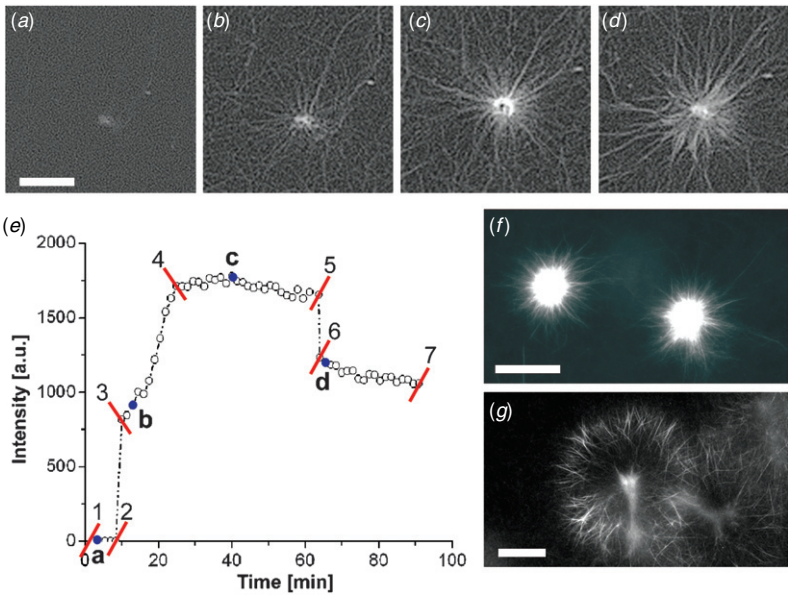

Figure 4. Evolution dynamics and novas of rings and asters. (*a*)–(*e*) The solution contains 21 μM G-actin, [F]/[A] = 0.05, and [M]/[A] = 0.1. Frames ((*a*) to (*d*)) represent consecutive temporal evolution stages of a ring taken after: (*a*) 2 min, (*b*) 15 min, (*c*) 42 min and (*d*) 1 h 5 min. Bar = 25 μm. (*e*) Temporal evolution of the ring measured by the fluorescence intensity of the labeled actin. Six evolution stages are distinguished: 1–2, 2–3, 3–4, 4–5, 5–6 and 6–7; the blue dots correspond to the stages depicted in (*a*)–(*d*). Asters before (*f*) and after (*g*) nova. Conditions: [A] = 21 μM, [F]/[A] = 0.1 and [M]/[A] = 0.1. Bar = 20 μm.

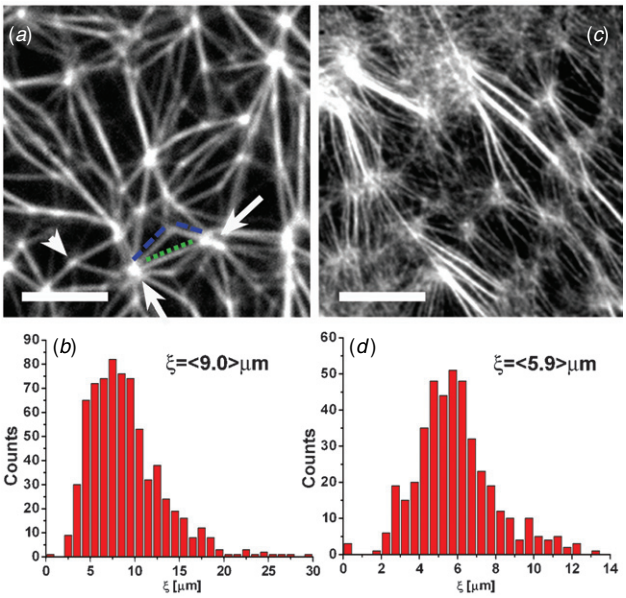

Figure 5. Active networks: long scale dynamics. The solution contains [A] = 21 μM, [F]/[A] = 0.14, and [M]/[A] = 0.056. Structure of the same dense active network few minutes (*a*) and 24 h (*c*) after mixing. (*a*) Arrows mark 'AJs' and the arrow-head marks a 'T' junction. The green dot and blue dash lines mark straight and V-shaped bundles, respectively, connecting the two 'AJs'. ((*a*) and (*c*)) Bar = 10 μm. The inter-junction distance distribution function of the networks, a few minutes and 24 h after mixing, are given in (*b*) and (*d*), respectively.

of AFBs is clearly observed (figure 4(*c*)). The structure is stable for ∼40 min; then at segment 5–6, a sudden explosion (the explosion takes 18 s with a rate of intensity decrease of 730 au min^{-1}) is detected during which expulsion of actin from the ring annulus occurs (figure 4(*d*)), leading to a sharp decrease in the local actin density (figure 4(*e*)). We call this phenomenon a 'ring nova'. In segment 6–7, the fluorescence intensity after the nova remains constant. The nova is not unique to rings; it also occurs if the AFBs are organized into asters (figure 4(*f*)) as seen in figure 4(*g*). An 'aster nova' typically occurs after 45–100 min and only in fully developed symmetric asters. The nova mechanism is not fully understood. Yet, we expect that additional motors from the surrounding medium continue to attach to the astral and ring AFBs ('track' AFBs). After getting attached, these motors move toward the aster center or ring annulus in a direction determined by the polarity of the 'track' AFBs. The accumulation of myosin II motors at the aster core or ring annulus can lead to the build-up of a critical mechanical stress sufficient for a nova. If the motors accumulate to the ring annulus, we infer that, as for asters, the 'minus' end of the AFBs emanating from the ring core points away from the ring center.

3.3.2. Structural evolution of active networks. Dense active networks initially reorganize on a time scale of minutes (figures 2(*g*), (*k*) and 5(*a*), and movies 1 and 2 available at stacks.iop.org/PhysBio/3/264) and generate highly stable structures unchanged for hours. This means that the initial self-organization process of dense active networks halts when the system reaches a mechanical stable state, signifying that the forces developed within the structure due to the action of the myosin II motors are balanced. In figure 5(*a*) we zoom in on a network a few minutes after mixing and 24 h later (figure 5(*c*)). Initially, the network is composed of 'AJs' (arrows) connected by straight (green dot line) or V-shaped (blue dash line) bundles. After 24 h, the bundles between network junctions are straight and appear to be under tension. Their overall number has increased significantly while their width has been reduced, suggesting that bundle splitting has occurred. Interestingly, the average inter-junction distance, ξ, is reduced from ξ = 9.0 μm (figure 5(*b*)) to less then ξ = 5.9 μm (figure 5(*d*)), which is the average value of the distance between the well-defined bundles.

The long-term structural rearrangements in active networks and in asters and rings may be attributed to the accumulation of motors (and therefore of stresses) at the junction points. However, in active networks the structural rearrangements appear only many hours after mixing and are not detected during the regular time scale (∼2 h) of the experiments, as happens for asters and rings. But in contrast to rings and asters, network reorganizations can also result from ATP depletion[4], which affects the binding properties of the motors and increases the force generated per motor head [44].

3.4. Asters and networks, and rings—proposed models

3.4.1. Junctions and intersection. In the following, we propose a simplified schematic model for explaining the architecture of asters and networks. Myosin II motors are 'plus' end motors. Thus, in networks and asters, when AFBs intersect, the myosin II motors move toward the 'plus' end of the AFBs. In isolated asters all the intersecting AFBs are freely carried by motors until they reach the end of the track to create the aster core (figures 6(*a*) and (*f*)). In the case of networks, the carried AFB is occasionally connected at one end to the surrounding network and therefore might stall before the track end; the result is that in contrast to asters where all the AFBs 'plus' ends are connected at the aster core, in networks there are three types of meeting points between AFBs: (a) 'aster junction' ('AJ') where all the AFBs' 'plus' ends meet at the junction point (figures 6(*a*) and 5(*a*), arrows); (b) 'T junction' (T) where the 'plus' end of an AFB is connected to the middle of another AFB (figures 6(*b*) and 5(*a*), arrow-head); (*c*) 'Intersection point' (X) of two AFBs somewhere in their middle (figure 6(*c*)). This type of intersection can further transform to parallel and anti-parallel bundling of AFBs depending on the direction of an applied force F (figures 6(*c*)–(*e*)). The force F, which in this case is a pulling force, represents the internal forces that develop within the network structure by the action of the myosin II motors.

[4] ATP concentration is kept constant (at saturating mM concentration) via an ATP regenerating system, see section 2. After several hours the efficiency of this system may change; as a result ATP concentration can decrease.

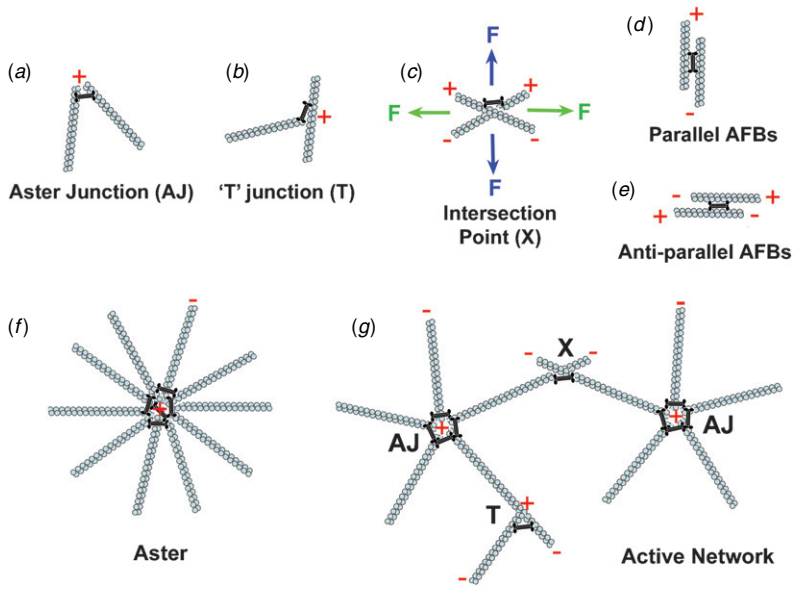

Figure 6. Asters and networks schematic diagram. Three types of junctions can be formed when two AFBs intersect. (*a*) 'AJ' where all the AFBs 'plus' ends meet at the junction point. (*b*) 'T' junction where the 'plus' end of an AFB is connected to the middle of another AFB. (*c*) 'X' junction of two AFBs not at their ends. An 'X' junction can transform into straight parallel (*d*) or anti-parallel (*e*) composite AFBs depending on the direction of an applied force *F*. (*f*) Structure of an 'aster'. The 'plus' ends of all the AFBs (marked by a '+' symbol) are pointing toward the aster core. (*g*) The basic structure of an 'active network' is given. Such a network is composed of 'AJs' connected by AFBs which are held together in a V-shape anti-parallel manner by myosin II motor (this forms a 'X' junction). The '+' and '−' ends mark the AFBs polarity within the network.

3.4.2. Interconnections between 'aster junctions' in a network. In 'active networks' one can identify many interconnections between 'AJs'. These junctions are usually very bright and the AFBs emerge from the junction in all directions (figure 5(*a*), arrows). The formation of networks begins with the polymerization and the bundling of actin filaments by fascin to form AFBs. Following polymerization, the AFBs start to overlap and myosin II motors initiate relative movement between the AFBs at their meeting points. This relative transport can result in an 'AJ' as long as the degree of interconnectivity (early times) between the AFBs is low and the network is relatively loose, therefore enabling free transport of AFBs (figures 6(*a*) and (*f*)). With time, the degree of interconnectivity increases; the AFBs' mobility becomes more restricted, leading to the formation of 'T' and 'X' junctions. The interconnections between the 'AJs' are either straight (green dot line, figure 5(*a*)) or V-shape (blue dash line, figure 5(*a*)) and are composed of individual AFBs (originating from two distinct 'AJs') held together by myosin II motors. Since the 'plus' ends of the AFBs forming an 'AJ' point toward the junction core, we expect that in a straight shape connection the two original AFBs are organized in an anti-parallel manner, with the 'minus' end of the AFBs pointing away from their 'AJ' centers. Such anti-parallel connected AFBs can be formed by the process indicated by the green arrows in figure 6(*c*). In fact, every connection between two 'AJs' involves an anti-parallel 'X' junction as described in figure 6(*g*). This 'X' junction can have a V-shape with a variable angle depending on the pulling forces exerted by the surrounding network. In practice, the movement of myosin II motors toward the 'plus' ends of the AFBs induces a relative sliding movement between these anti-parallel AFBs, resulting in a reduction of the distances between the 'AJs'. This anti-parallel organization explains the experimentally observed network contractions in dense active networks (figures 5(*c*) and (*d*)).

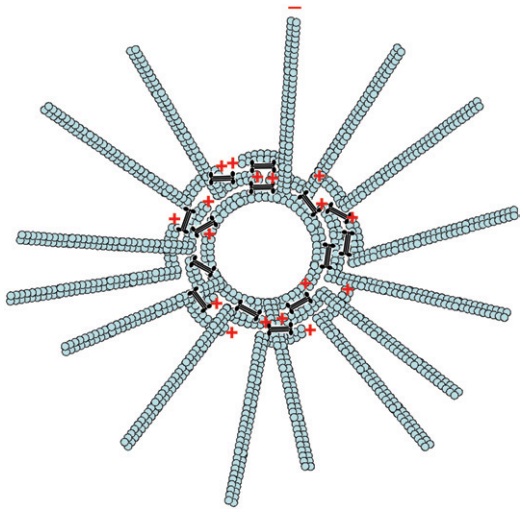

Figure 7. Ring schematic diagram. The ring self-organizes from the surrounding network. Since the myosin II are 'plus' end motors, the AFBs emanating from the ring structure have their 'minus' (marked by a '−' symbol) ends pointing away from its center. The polarity of the AFBs within the ring annulus is arbitrary; the AFBs' 'plus' ends (marked by a '+' symbol) are randomly distributed within the ring circumference.

3.4.3. Rings. Unlike asters, which are made of rigid AFBs, rings are formed at fascin concentrations that are rather low ([F]/[A] = 0.05). Under these conditions, the bundles are rather flexible and the forces applied by the motors during the reorganization process can induce their curving. The rings evolve from the surrounding network through the action of the motors. This action results in organization of the AFBs so that their minus ends point outward. While the 'minus' ends are loose and are pointing to the surrounding network, the 'plus' ends are bent and curved to form the ring structure. *A priori* there is no reason for the AFBs to face in a certain direction (clockwise or anticlockwise) along the ring circumference; therefore statistically, the number of 'clockwise' and 'anticlockwise' AFBs should be equal (figure 7).

4. Conclusion and outlook

Here we show that for actin, myosin and fascin, the presence of ATP is sufficient to produce a wide variety of large scale structures. In this *in vitro* system, the bundling activity of fascin is required to obtain significant organization; without fascin the system does not self-organize to produce any patterns that can be optically resolved, regardless of motors concentration. *In vivo*, fascin is essential for the formation of stress fibers [6] and filopodia protrusions [38]. Therefore our *in vitro* assay opens the way to a systematic analysis of the synergistic role of motor and bundling proteins.

Our results demonstrate that moderate motor concentrations drive the formation of cytoskeletal structures, but above a critical motor concentration the forces generated by the motors are large enough to break the structures (see figure 2(*l*) and the supplementary figure available at stacks.iop.org/PhysBio/3/264). At even higher motor concentrations, the formation and growth of AFBs is inhibited, and therefore the self-organization does not even start. This can be attributed to the ability of the motors to sever bundles [45] or to affect actin assembly/disassembly dynamics [46–48]. We can therefore conclude that actin self-organization is possible only when the AFBs attain a certain length and mechanical stability to be pulled, transported and deformed by myosin II motors without breaking or depolymerizing. Eventually, the complex interplay between myosin II and bundling protein activities determines the mechanical properties of the bundles and in turn, the type of the resulting patterns. For this reason curved structures such as rings are observed at low fascin concentrations where the bundles are composed of a small number of actin filaments (data not shown) and are therefore rather flexible [49]. In contrast, at higher fascin concentrations where the bundles are thicker and the forces applied during active transportation by myosin II are not capable of bending them, the self-organization produces structures such as asters and dense crosslinked networks.

The active patterns shown here and their dynamics of formation involve totally different mechanisms compared to passive systems [43]. We can therefore expect that the viscoelastic properties as well as the time scales characterizing these active gels will be totally different from those observed in passive solutions of actin filaments [15–18] or solutions of actin supplemented with passive crosslinkers [43, 50]. Our findings are the first to show a full phase diagram of such an active system and present a wide range of active processes and dynamics, many of them not predicted by current theoretical models. We observe a reorganization process at low motor concentrations that seems to reach its final steady state after ∼30 min. However, at higher motor concentrations there is a reorganization process on short time scales and a further structural transformation on longer time scales which results in 'novas' in rings or asters and contractions in the case of network structures. We suggest that the transformation process in rings and asters is the result of the growing number of free motors in the solution that slowly accumulate at the ring annulus or aster center and produce a growing mechanical force, eventually sufficient to break the whole pattern. However, in the case of networks the build-up of stresses at the junction points may also result from a change in the forces generated by each motor head.

Here we bring the first *in vitro* experimental evidence of the capability of myosin II motors to self-organize actin into rings. Moreover this is demonstrated in a membrane-free system, where the ring is assembled by active transportation of AFBs from the surrounding bulk. This proves that rings can be formed just by optimizing the local concentration of actin, bundling proteins and motors. In cells the formation of a contractile ring occurs in the vicinity of the plasma membrane by locally nucleating actin filaments by formin [51, 52], but as we see from this *in vitro* system, the ring assembly does not require the presence of the membrane for determining its final shape.

While *in vitro* the rings do not dynamically disassemble, *in vivo* the contractile ring continuously disassembles during contraction and therefore maintains a constant density of actin and protein composition, in contrast to myosin II concentration, which locally increases [8]. We can speculate that *in vivo* there is a delicate coupling between actin severing and depolymerization, and ring contraction rates, or even that there is a control mechanism that is responsible for adjusting the actin disassembly/severing rate during the ring contraction. This control mechanism involves other proteins, e.g. ADF/cofilin, known to regulate actin disassembly [8, 53]. Myosin II may participate in this regulation mechanism too. Such a mechanism is essential for preventing accumulation of stresses leading to catastrophe, or 'novas', as was observed here in rings.

Finally, here we show that myosin II motors above a critical concentration can disassemble mesoscopic structures or even prevent actin polymerization. *In vivo*, the cytoskeletal structures (i.e. contractile ring, stress fibers) are dynamic; they assemble and disassemble as a function of the cell's needs. Our results demonstrate that one possible mechanism regulating the disassembly of these structures is simply tuning the concentration/activity of the myosin II motors.

To conclude, the work presented here is a first step toward understanding the patterning and self-organization of active gels. In this work, we studied the patterning of actin by myosin

II motors in the presence of fascin; here, the reorganization process results essentially from myosin II activity and not from actin treadmilling. In general, the patterning process is expected to result from interplay between actin polymerization and bundling rates, and myosin II motor action. Future works will have to test parameters not studied in this work. For instance, it will be interesting to test different types of bundling proteins. In addition, there is a need to study the role of ATP concentration (ATP concentration affects the velocity of the motors as well as the force generated by the motors), as well as actin treadmilling. We expect that an increase in actin treadmilling or ATP concentration will increase the intrinsic 'activity' of the system and as a result will affect the dynamics of reorganization as well as the type of patterns generated. We also hope that this study will stimulate theoretical work and efforts to better understand the mechanisms of active gel reorganization. We hope that using these models, we will be able to test the validity of our proposed mechanisms for aster, network and ring formation.

Acknowledgments

This work was supported by the Reimund Stadler Minerva Center and by the research grants from the Israel Cancer Association (ICA grant 20040070) and the Israel Science Foundation (ISF grant 551/04). We thank Frank Jülicher for useful comments and David Gillo for a careful reading of the manuscript.

Glossary

Myosin II motors. This class of motors has a unique property to spontaneously self-assemble into small motor aggregates commonly named 'minifilaments' that can simultaneously interact with a number of actin filaments and move toward their 'plus' end in the presence of ATP. As a result myosin II motors play a central role in many cellular processes such as cell division, contraction and motility.

Active versus passive crosslinkers. Passive crosslinker are proteins that attach and detach from cytoskeletal filaments without producing any force or work. Active crosslinking proteins (i.e., myosin II motor proteins), on the other hand, are active elements that can generate force and relative movement between filaments.

Active processes. Active processes are processes that are driven by the chemical energy of ATP hydrolysis such as force generation by molecular motor proteins or forces resulting from the polymerization/depolymerization kinetics of cytoskeletal filaments. If such active processes take place in a system, thermodynamic equilibrium cannot be reached. Under these conditions, the forces and motions generated at the molecular level modify the properties of this active material as compared to corresponding passive system; an example of such material is the cell cytoskeleton.

Aster and ring 'novas'. Aster and rings are example of two types of large scale patterns (i.e., structures) that are formed when mixing actin, myosin II motors and fascin. The formation of these structures is driven by the action of the myosin II motors which act as the reorganizing center. Aster and ring novas have been observed experimentally and are manifested in an abrupt disruption of the structure.

References

[1] Fabry B, Maksym G N, Butler J P, Glogauer M, Navajas D, Tabak N A, Millet E J and Fredberg J J 2003 Time scale and other invariants of integrative mechanical behavior in living cells *Phys. Rev.* E **68** 0419141–18

[2] Deng L, Trepat X, Butler J P, Millet E, Morgan K G, Weitz D A and Fredberg J J 2006 Fast and slow dynamics of the cytoskeleton *Nature Mat.* **5** 636–40

[3] Pollard T D and Borisy G G 2003 Cellular motility driven by assembly and disassembly of actin filaments *Cell* **112** 453–65

[4] Wang Y L 1985 Exchange of actin subunits at the leading edge of living fibroblasts: possible role of treadmilling *J. Cell Biol.* **101** 597–602

[5] Howard J 1997 Molecular motors: structural adaptations to cellular functions *Nature* **389** 561–7

[6] Yamashiro-Matsumura S and Matsumura F 1986 Intracellular localization of the 55-kD actin-bundling protein in cultured cells: spatial relationships with actin, alpha-actinin, tropomyosin, and fimbrin *J. Cell. Biol.* **103** 631–40

[7] Pelham R J and Chang F 2002 Actin dynamics in the contractile ring during cytokinesis in fission yeast *Nature* **419** 82–6

[8] Wu J-Q and Pollard T D 2005 Counting cytokinesis proteins globally and locally in fission yeast *Science* **310** 310–4

[9] Ingber D E 2003 Tensegrity I: cell structure and hierarchical systems biology *J. Cell Sci.* **116** 1157–73

[10] Verkhovsky A B, Svitkina T M and Borisy G G 1997 Polarity sorting of actin filaments in cytochalasin-treated fibroblasts *J. Cell. Sci.* **110** 1693–704

[11] Hyman A and Karsenti E 1996 Morphogenetic properties of microtubules and mitotic spindle assembly *Cell* **84** 401–10

[12] Verkhovsky A B, Svitkina T M and Borisy G G 1995 Myosin II filament assemblies in the active lamella of fibroblasts: their morphogenesis and role in the formation of actin filament bundles *J. Cell. Biol.* **131** 989–1002

[13] Kaminer B and Bell A L 1980 Myosin filamentogenesis: effect of pH and ionic concentration *J. Mol. Biol.* **20** 391–401

[14] Dean S O, Rogers S L, Stuurman N, Vale R D and Spudich J A 2005 Distinct pathways control recruitment and maintenance of myosin II at the cleavage furrow during cytokinesis *Proc. Natl Acad. Sci.* **102** 13473–8

[15] Gittes F, Schnurr B, Olmsted P D, MacKintosh F C and Schmidt C F 1997 *Phys. Rev. Lett.* **79** 3286

[16] Amblard F, Maggs A C, Yurke B, Pargellis A and Leibler S 1996 Subdiffusion and anomalous local viscoelasticity in actin networks *Phys. Rev. Lett.* **76** 4470–3

[17] Liu J, Gardel M L, Kroy K, Frey E, Hoffman B D, Crocker J C, Bausch A R and Weitz D A 2006 Microrheology probes length scale dependent rheology *Phys. Rev. Lett.* **96** 118104

[18] Wong I Y, Gardel M L, Reichman D R, Weeks E R, Valentine M T, Bausch A R and Weitz D A 2004 Anomalous diffusion probes microstructure dynamics of entangled F-actin networks *Phys. Rev. Lett.* **92** 1781011–4

[19] Legoff L, Amblard F and Furst E 2002 Motor-driven dynamics in actin-myosin networks *Phys. Rev. Lett.* **88** 018101

[20] Humphrey D, Duggan C, Saha D, Smith D and Kas J 2002 Active fluidization of polymer networks through molecular motors *Nature* **416** 413–6

[21] Lau A W, Hoffman B D, Davies A, Crocker J C and Lubensky T C 2003 Microrheology, stress fluctuations, and active behavior of living cells *Phys. Rev. Lett.* **91** 1981011–4
[22] Surrey T, Nedelec F, Leibler S and Karsenti E 2001 Physical properties determining self-organization of motors and microtubules *Science* **292** 1167–71
[23] Nedelec F, Surrey T, Maggs A C and Leibler S 1997 Self-organization of microtubules and motors *Nature* **389** 305–8
[24] Takiguchi K 1991 Heavy meromyosin induces sliding movements between antiparallel actin filaments *J. Biochem. (Tokyo)* **109** 520–7
[25] Tanaka-Takiguchi Y *et al* 2004 The elongation and contraction of actin bundles are induced by double-headed myosins in a motor concentration-dependent manner *J. Mol. Biol.* **341** 467–76
[26] Bernheim-Groswasser A, Wiesner S, Golsteyn R M, Carlier M-F and Sykes C 2002 The dynamics of actin-based motility depend on surface parameters *Nature* **417** 308–11
[27] Haviv L *et al* 2006 Reconstitution of the transition from lamellipodium to filopodium in a membrane-free system *Proc. Natl Acad. Sci.* **103** 4906–11
[28] Loisel T P, Boujemaa R, Pantaloni D and Carlier M-F 1999 Reconstitution of actin-based motility of *Listeria* and *Shigella* using pure proteins *Nature* **401** 613–316
[29] Vignjevic D, Yarar D, Welch M D, Peloquin J, Svitkina T and Borisy G G 2003 Formation of filopodia-like bundles *in vitro* from a dendritic network *J. Cell Biol.* **160** 951–62
[30] Liverpool T B and Marchetti M C 2003 Instabilities of isotropic solutions of active polar filaments *Phys. Rev. Lett.* **90** 138102
[31] Kruse K, Joanny J F, Julicher F, Prost J and Sekimoto K 2004 Asters, vortices, and rotating spirals in active gels of polar filaments *Phys. Rev. Lett.* **92** 078101–4
[32] Aranson I S and Tsimring L S 2005 Pattern formation of microtubules and motors: inelastic interaction of polar rods *Phys. Rev.* E **71** 050901
[33] Lee Y H and Kardar M 2001 Macroscopic equations for pattern formation in mixtures of microtubules and molecular motors *Phys. Rev.* E **64** 0561131–8
[34] Voituriez R, Joanny J F and Prost J 2006 Generic phase diagram of active polar films *Phys. Rev. Lett.* **96** 0281021–4
[35] Bausch A R and Kroy K 2006 *Nature Phys.* **2** 231–8
[36] Janson E W, Kolega J and Taylor D L 1991 Modulation of contraction by gelation/solation in a reconstituted motile model *J. Cell. Biol.* **114** 1005–15
[37] Ishikawa R, Sakamoto T, Ando T, Higashi-Fujime S and Kohama K 2003 Polarized actin bundles formed by human fascin-1: their sliding and disassembly on myosin II and myosin V *in vitro J. Neurochem.* **87** 676–85
[38] Vignjevic D, Kojima S, Aratyn Y, Danciu O, Svitkina T and Borisy G G 2006 Role of fascin in filopodia protrusion *J. Cell Biol.* **174** 863–75
[39] Spudich J A and Watt S 1971 The regulation of rabbit skeletal muscle contraction: I. Biochemical studies of the interaction of the tropomyosin–troponin complex with actin and the proteolytic fragments of myosin *J. Biol. Chem.* **246** 4866–71
[40] Margossian S S and Lowey S 1982 Preparation of myosin and its subfragments from rabbit skeletal muscle *Methods Enzymol* **85** 55–71
[41] Recombinant Fascin was prepared by a modification of the method of Ono, S *et al* 1997 Identification of an actin binding region and a protein kinase C phosphorylation site on human fascin *J. Biol. Chem.* **272** 2527–33
[42] Perret E, Leung A, Morel A, Feracci H and Nassoy P 2002 Versatile decoration of glass surfaces to probe individual protein–protein interactions and cellular adhesion *Langmuir* **18** 846–54
[43] Tseng Y, Fedorov E, McCaffery J M, Almo S C and Wirtz D 2001 Micromechanics and ultrastructure of actin filament networks crosslinked by human fascin: a comparison with alpha-actinin *J. Mol. Biol.* **310** 351–66
[44] Debold E P, Patlak J B and Warshaw D M 2005 Slip sliding away: load-dependence of velocity generated by skeletal muscle myosin molecules in the laser trap *Biophys. Lett.* L34–6
[45] Medeiros N A, Burnette D T and Forscher P 2006 Myosin II functions in actin-bundle turnover in neuronal growth cones *Nat. Cell Biol.* **8** 215–26
[46] Guha M, Zhou M and Wang Y 2005 Cortical actin turnover during cytokinesis requires myosin II *Curr. Biol.* **15** 732–6
[47] Murthy K and Wadsworth P 2005 Myosin-II-dependent localization and dynamics of F-actin during cytokinesis *Curr. Biol.* **15** 724–31
[48] Burgess D R 2005 Cytokinesis: new roles for myosin *Curr. Biol.* **15** R310–1
[49] Mogilner A and Rubinstein B 2005 The physics of filopodial protrusion *Biophys. J.* **89** 782–95
[50] Shin J H, Gardel M L, Mahadevan L, Matsudaira P and Weitz D A 2004 Relating microstructure to rheology of a bundled and cross-linked F-actin network *in vitro Proc. Natl Acad. Sci.* **101** 9636–41
[51] Piekny A, Werner M and Glotzer M 2005 Cytokinesis: welcome to the Rho zone *Trends Cell Biol.* **15** 651–8
[52] Balasubramanian M K, Bi E and Glotzer M 2004 Comparative analysis of cytokinesis in budding yeast, fission yeast and animal cells *Curr. Biol.* **14** R806–18
[53] Nakano K and Mabuchi I 2006 Actin-depolymerizing protein Adf1 is required for formation and maintenance of the contractile ring during cytokinesis in fission yeast *Mol. Biol. Cell.* **17** 1933–45